

## Article

# Absorption and Distribution of Calcium ( $^{45}\text{Ca}$ ) Applied to the Surface of Orange (*Citrus sinensis*) Fruits at Different Developmental Stages

Claudia Bonomelli <sup>1</sup>, Victoria Fernández <sup>2</sup>, Franco Capurro <sup>1</sup>, Carola Palma <sup>1</sup>, Ximena Videla <sup>3</sup>, Ximena Rojas-Silva <sup>3</sup>, Adriana Nario <sup>3</sup> and Johanna Mártiz <sup>1,\*</sup>

<sup>1</sup> Departamento de Fruticultura y Enología, Facultad de Agronomía e Ingeniería Forestal, Pontificia Universidad Católica de Chile, Vicuña Mackenna 4860, Macul, Santiago 7820436, Chile; cbonomel@uc.cl (C.B.); facapurro@uc.cl (F.C.); cppalma@uc.cl (C.P.)

<sup>2</sup> Departamento de Sistemas y Recursos Naturales, Escuela Técnica Superior de Ingenieros Forestales, Universidad Politécnica de Madrid, 28040 Madrid, Spain; v.fernandez@upm.es

<sup>3</sup> División de Investigación y Desarrollo, Comisión Chilena de Energía Nuclear, Santiago 7600713, Chile; ximena.videla@cchen.cl (X.V.); ximena.rojas@cchen.cl (X.R.-S.); adriana.nario@cchen.cl (A.N.)

\* Correspondence: jmartiz@uc.cl; Tel.: +56-2-2354-4159



**Citation:** Bonomelli, C.; Fernández, V.; Capurro, F.; Palma, C.; Videla, X.; Rojas-Silva, X.; Nario, A.; Mártiz, J. Absorption and Distribution of Calcium ( $^{45}\text{Ca}$ ) Applied to the Surface of Orange (*Citrus sinensis*) Fruits at Different Developmental Stages. *Agronomy* **2022**, *12*, 150. <https://doi.org/10.3390/agronomy12010150>

Academic Editors: Othmane Merah, Purushothaman Chirakkuzhyil, Abhilash, Magdi T. Abdelhamid, Hailin Zhang and Bachar Zebib

Received: 7 December 2021

Accepted: 6 January 2022

Published: 8 January 2022

**Publisher's Note:** MDPI stays neutral with regard to jurisdictional claims in published maps and institutional affiliations.



**Copyright:** © 2022 by the authors. Licensee MDPI, Basel, Switzerland. This article is an open access article distributed under the terms and conditions of the Creative Commons Attribution (CC BY) license (<https://creativecommons.org/licenses/by/4.0/>).

**Abstract:** In this study, the rate of absorption and transport of calcium (Ca) in orange fruits (*Citrus sinensis* cv. Fukumoto) after surface treatment with  $^{45}\text{Ca}$  was evaluated by supplying treatments at different dates between fruit set and mid-phase II of growth (i.e., 30, 44, 66 and 99 days after full bloom, DAFB).  $^{45}\text{Ca}$  absorption was always detected, but  $^{45}\text{Ca}$  application at the fruit set was associated with the highest rates of Ca transport into the pulp (39%) compared to the other treatments (17–19%). Scanning electron microscopy (SEM) images of the fruit surface showed the occurrence of stomata along with the entire rind at all the developmental stages evaluated. However, from the beginning of stage I, stomata began to collapse and develop plugs, and this became frequent as the fruit age increased. From 44 DAFB, oil gland density increased, and Ca oxalates (CaOx) were found in the fruit flavedo and albedo. Fruit Ca (not labeled) concentration increased from fruit set (30 DAFB) to 99 DAFB, although oil gland formation and rind growth and differentiation likely hindered Ca transport to internal fruit tissues (pulp). The total Ca concentration in the pedicel was always higher than that in the fruit, with no differences between the first three treatments. The information obtained in this study may be essential for improving Ca fertilizer efficacy in citrus by spray applications.

**Keywords:** calcium; foliar application; fruit; morphology; orange

## 1. Introduction

Calcium (Ca) has different functions in plants, such as being a structural component of the cell wall and a cytosolic messenger in cells [1]. Calcium uptake by plants from soil occurs through the roots, and its accumulation in fruit is dependent on transport through the xylem, as calcium has low phloem mobility [1,2]. The Ca content in fruit is highly regulated by transpiration [3,4], showing greater content in organs with more transpiration, such as leaves [5]. Therefore, the lower transpiration capacity of fruits compared to leaves makes them more susceptible to Ca deficit [1]. Calcium influx and accumulation into the fruit have been reported to be higher during the early stages of development and decrease progressively over time [6]. This effect is likely due to the higher transpiration rates at the early stages of fruit development, which are closely related to Ca accumulation in fruit [2,4,5].

Many disorders have been related to Ca nutrition, but the mechanisms that control their occurrence are not clearly understood yet. Any condition that affects Ca uptake by the plant and its distribution to the fruit can lead to Ca deficit disorder [7–10]. In

citrus fruits, a variety of disorders related to Ca availability exist, the most common being cracking [3], albedo breakdown [11], splitting, and peel pitting [12]. Calcium disorders are mainly caused by the low mobility of Ca and cellular Ca partitioning in the plant or tissue, but it is also possible to have Ca-related disorders associated with a high Ca content in a given tissue [1,7].

Foliar Ca applications are a common way to supply Ca to the fruit, but the supplied Ca mostly stays within the treated plant part, with a small proportion moving to adjacent organs [13]. These foliar Ca applications commonly aim at improving firmness and color and decreasing fruit disorders [3,7,11]. Fernández et al. [14] showed that the effectiveness of foliar applications depends on various aspects such as environmental factors such as temperature and humidity; physicochemical factors such as concentration, solubility, charge, and solution pH; or plant-related factors such as the presence of trichomes [15], stomata [16], the nature of the cuticle, or plant physiological status [17].

Regarding morphological factors, the cuticle is the first barrier against the absorption of foliar-applied chemicals [18]. Thus, cuticular irregularities, such as cracks or the presence of stomata or trichomes can significantly contribute to foliar uptake [17]. According to Wang et al. [19], the cuticle develops over time; in Newhall oranges, it has a minimal presence until 90 days after full bloom (DAFB) and reaches its maximum thickness at approximately 150 DAFB. As the cuticle grows, wax platelets start forming all over the fruit cuticle surface to the point where stomata are plugged by them [20,21]. Stomata have been shown to collapse and lose functionality as the season advances [20].

Citrus fruits have three main parts that are morphologically distinct, i.e., flavedo, albedo, and pulp [22]. The exocarp or flavedo, which is the colored external part of the rind, contains stomata and oil glands in its epidermis. The flavedo surface is covered by a cuticle, and its width depends mainly on the age of the fruit, which thickens over time [22–24]. During the early stages, flavedo is a photosynthetically active tissue with chloroplasts that are transformed into chromoplasts while the fruit ripens [25].

The mesocarp or albedo is the inner part of the rind, typically being white or uncolored. Fruit size increases mostly during stage I due to growth of the mesocarp, representing 90% of the fruit volume, but in stage II, this growth stops [25,26]. In this stage, the albedo develops numerous air spaces, increasing its intercellular space [22]. As the pulp grows, the albedo becomes thinner [25]. Finally, the pulp conforms to the edible part of the fruit. These vesicles begin formation after bloom [22,26]. The juice sac number shows little increase during stage I of fruit development, and in stage II, the pulp grows due to cell expansion [24,25].

Fruit morphological tissues have been shown to exhibit different Ca influx behaviors and Ca concentrations [6]. Some tissues even have shown the capacity to form calcium oxalate (CaOx) crystals in the vacuole of specialized cells called idioblasts [27,28], effectively sequestering calcium [29,30]. Crystal formation is believed to be a genetically regulated process, and large amounts of Ca be precipitated as CaOx, which is physiologically and osmotically inactive [28]. This process reduces the apoplastic concentration of Ca in adjacent cells [31] and regulates the cytosolic calcium level to avoid interference with cell processes [32,33]. Despite high fruit calcium concentrations, fruit can show deficiency symptoms when calcium is sequestered as calcium oxalate [6].

A common technique to study Ca absorption, distribution, and partitioning among organs and tissues is the use of Ca-45 (<sup>45</sup>Ca) as a tracer [34–38]. Studies using Ca isotopes have shown that the absorption of calcium directly applied to the fruit is positively correlated with its distribution in the fruit's inner tissues [13,39]. This study aimed to evaluate the link between navel orange fruit morphology (from fruit set to mid-stage II) and the absorption and mobility of surface-applied Ca using <sup>45</sup>Ca as a tracer.

## 2. Materials and Methods

### 2.1. Site and Plant Material

The experiment was carried out in Central Chile (−33.77 Lat. and −70.73 Lon.) in a ten-year-old orange orchard (*Citrus sinensis* L. Osbeck cv. Fukumoto) on (*Poncirus trifoliata*) Rubidoux rootstock. The soil was classified as fluventic haploxerolls according to USDA soil taxonomy; the soil Ca concentration (24 cmol+/kg) was measured by extraction with 1 N ammonium acetate at pH 7.0 and analyzed by inductively coupled plasma—optical emission spectroscopy (ICP-OES, Agilent 720 ES axial spectrometer, Varian Inc., Victoria, Australia).

### 2.2. <sup>45</sup>Ca Measurements

To study Ca absorption and movement over different stages of fruit development, <sup>45</sup>Ca was used as a tracer on different dates. The treatment (Table 1) consisted of the application of 5 µL of <sup>45</sup>Ca directly to fruit using a micropipette and no surfactant, with <sup>45</sup>Ca Cl<sub>2</sub> (2,187,630 Bq m/L; PerkinElmer) at 5 mCi. Solutions were applied 30, 44, 66, and 99 days after full bloom (DAFB). To determine the <sup>45</sup>Ca activity in fruit per tissue, the calcination method of <sup>45</sup>Ca samples for isotope ratio analysis via liquid scintillation was used [40]. In April 2019, all treated fruit was harvested. Fruits (15) were collected at each developmental stage, and the diameter (mm) was determined.

**Table 1.** Description of the application times to the <sup>45</sup>Ca tracer. Days after full bloom (DAFB), dates, development stages, fruit diameter, and environmental conditions.

Treatment DAFB	Date	Development Stage	Fruit Diameter (mm)	Relative Humidity (%)	Air Temperature (°C)
30	11/14/18	Fruit Set	7.6 ± 0.9	69.5	13.5
44	11/28/18	Stage I	15.4 ± 1.9	66.5	16.0
66	12/20/18	End Stage I	29.2 ± 1.7	71.2	11.6
99	01/22/19	Mid Stage II	48.8 ± 1.7	64.9	17.8

### 2.3. Tissue Ca Concentrations

In each development stage, five fruits were collected, and the concentration of Ca (not labeled) in the pedicel and whole fruit were determined. At harvest time, fruits were partitioned into different parts (flavedo, albedo, and pulp) and Ca was analyzed. For this purpose, fresh fruit tissue (fresh weight, FW) was kept in an oven at 65 °C for 48 h until reaching a constant weight (dry weight, DW). Calcium concentration was determined after dry tissue ashing at 500 °C (4 h), ash dissolution in 2 M HCl, and Ca determination by ICP-OES (Agilent 720 ES axial—Varian, Victoria, Australia).

### 2.4. Electron Microscopy Observations

To analyze the fruit surface and inner tissues, scanning electron microscopy (SEM) was used. Samples containing rinds and pulp of each treatment were prepared from control fruit of the same developmental stages as those treated with <sup>45</sup>Ca. The tissue was obtained from the equatorial zone of the cut fruit with a scalpel. The SEM sample preparation protocol was as follows: fixation of the fruit samples in 2.5% glutaraldehyde, dehydration in an increasing series of ethanol concentrations from 30% to 100%, critical point drying, and sputtering with gold.

Samples were subsequently observed with a scanning electron microscope (Hitachi TM 3000 model and LEO 1420VP model). The composition of CaOx and wax-like substances were determined with an energy-dispersive X-ray spectroscopy (EDX) system (Oxford instruments with INCA software) coupled to the SEM apparatus.

To determine cuticle presence and thickness, transmission electron microscopy (TEM) samples were prepared from the fruit rind at 30 DAFB and 44 DAFB. The samples were

prepared according to a previously reported method [41] to protect the cuticle from possible chemical deterioration. TEM samples were observed in a Philips Tecnai 12 microscope (Eindhoven, The Netherlands) at 80 kV. Fruit tissues, pedicel tissues, and cellular structure and dimensions were estimated by image analysis (ImageJ software) [42].

### 2.5. Statistical Analysis

The experimental design was completely random, with four treatments and five replicates. Data were statistically analyzed with Infostat software [43] using analysis of variance (ANOVA). When the F test was significant ( $p < 0.05$ ), means were separated by Tukey's test. Data regarding  $^{45}\text{Ca}$  detection were transformed to arcsin-sqrt before ANOVA. Dry weight, Ca concentrations, and fruit diameter are expressed as means  $\pm$  standard deviation (SD).

## 3. Results

### 3.1. Absorption and Movement of $^{45}\text{Ca}$

The results of orange tissue analyses after  $^{45}\text{Ca}$  application at different dates and collected in April 2019, namely, flavedo + albedo (rind) and pulp, are shown in Figure 1. In all the fruits of the different applications, the presence of  $^{45}\text{Ca}$  was detected, indicating that Ca absorption occurred. On all application dates, the largest Ca concentration was found in the rind (flavedo + albedo). The distribution of Ca found in the different tissues was significantly different for the application treatment at 30 DAFB (fruit set), compared to the other treatments applied at 44, 66, and 99 DAFB, which have no differences between them.

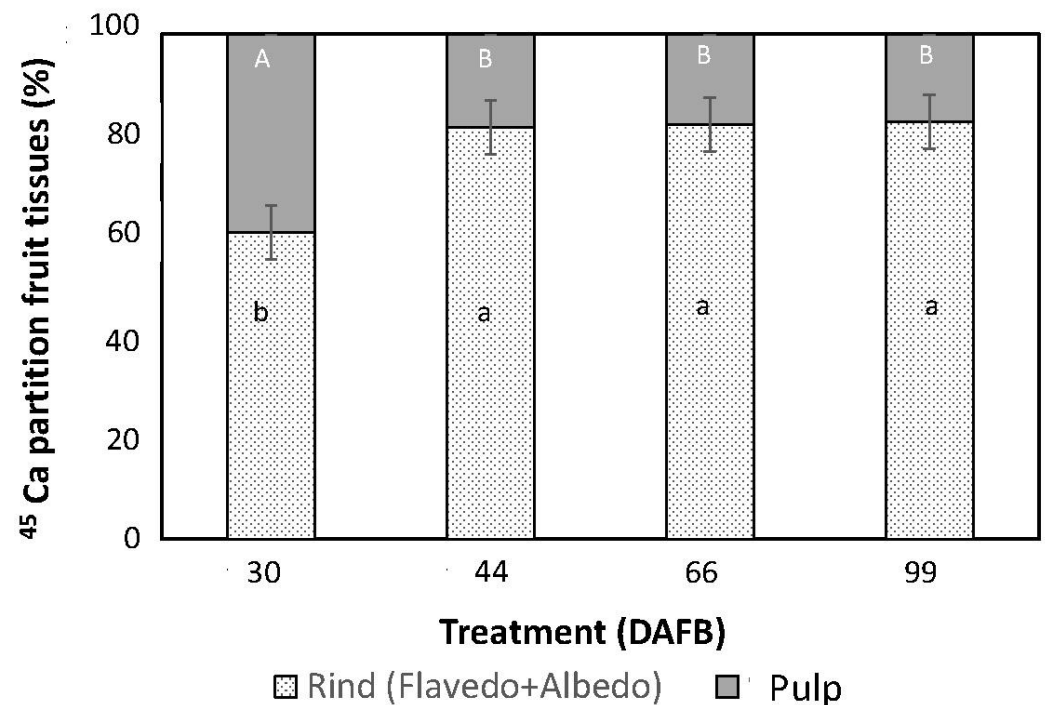


**Figure 1.**  $^{45}\text{Ca}$  partition at fruit harvest, pulp and rind (flavedo + albedo). Treatment:  $5\mu\text{L}$   $^{45}\text{Ca}$  application 30, 44, 66, and 99 days after full bloom (DAFB). Different capital and lower case letters indicate statistically significant differences ( $p \leq 0.05$ ) between treatment dates. Capital letters refer to differences regarding the rate of  $^{45}\text{Ca}$  partition in the pulp, and lowercase letters are associated with the rate of  $^{45}\text{Ca}$  partition in the rind.

In the pulp, the greatest Ca partition rate was observed for the 30 DAFB treatment (i.e., at fruit set,  $39 \pm 6\%$ ), which was significantly higher than at 44 DAFB ( $19 \pm 4\%$ ), 66 DAFB ( $18 \pm 2\%$ ), and 99 DAFB ( $17 \pm 3\%$ ) (Figure 1). Regardless of the date of application, the largest  $^{45}\text{Ca}$  concentration was always recovered in the rind (flavedo + albedo). The

$^{45}\text{Ca}$  partition rates in the flavedo were 29% at 30 DAFB and 39–45% at 44, 66 and 99 DAFB.  $^{45}\text{Ca}$  Calcium albedo partition varied from 31% at 30 DAFB and from 38–43% at 44, 66, and 99 DAFB.

### 3.2. Fruit Dry Weight and Ca Concentration

The dry weight of the fruit remained constant between 30 DAFB and 44 DAFB (Table 2). Between the beginning and end of phase I of fruit development, the dry weight decreased significantly. After the end of phase I, the dry weight decreased slightly (Table 2).

**Table 2.** Dry weight (D.W., %) and Ca concentration (% D.W.) in whole fruit and pedicel (data are means  $\pm$  standard deviations, SD). Within columns, values marked with different letters are significantly different according to Duncan's Multiple Range Test ( $p \leq 0.05$ ).

Developmental Stage	DAFB	D.W. (%)		Ca Concentration (% D.W.)	
		Fruit	Pedicel	Fruit	Pedicel
Fruit Set	30	33.60 $\pm$ 1.58 a	27.44 $\pm$ 0.15 a	0.31 $\pm$ 0.05 a	2.72 $\pm$ 0.15 a
Stage I	44	32.50 $\pm$ 1.36 a	26.89 $\pm$ 0.40 a	0.48 $\pm$ 0.06 b	2.74 $\pm$ 0.10 a
End stage I	66	26.47 $\pm$ 3.01 b	32.48 $\pm$ 5.91 a	0.80 $\pm$ 0.21 c	2.49 $\pm$ 0.40 a
Mid stage II	99	21.23 $\pm$ 2.62 b	49.05 $\pm$ 9.33 b	0.87 $\pm$ 0.06 d	1.73 $\pm$ 0.46 b

Fruit Ca concentration significantly increased during fruit development, reaching a maximum at the mid-stage II phase (Table 2). The Ca concentration in the pedicel was always higher than in the fruit. Pedicel Ca concentrations were higher and not statistically different than earlier developmental stages compared to the decrease recorded for mid-stage II. On the other hand, the pedicel D.W. increased with fruit maturity. Finally, at harvest, the Ca concentration (% D.W.) determined in different fruit parts corresponded to 0.96  $\pm$  0.05% for the flavedo, 0.87  $\pm$  0.06% for the albedo, and 0.40  $\pm$  0.03% for the pulp.

### 3.3. Fruit Anatomy

#### 3.3.1. Rind Surface Topography

Stomata were observed in the entire rind at any stage of orange fruit development. During the fruit set, stomata showed a domed projection over them. This stomatal crypt forms a protective chamber over the stomatal pore (Figure 2).

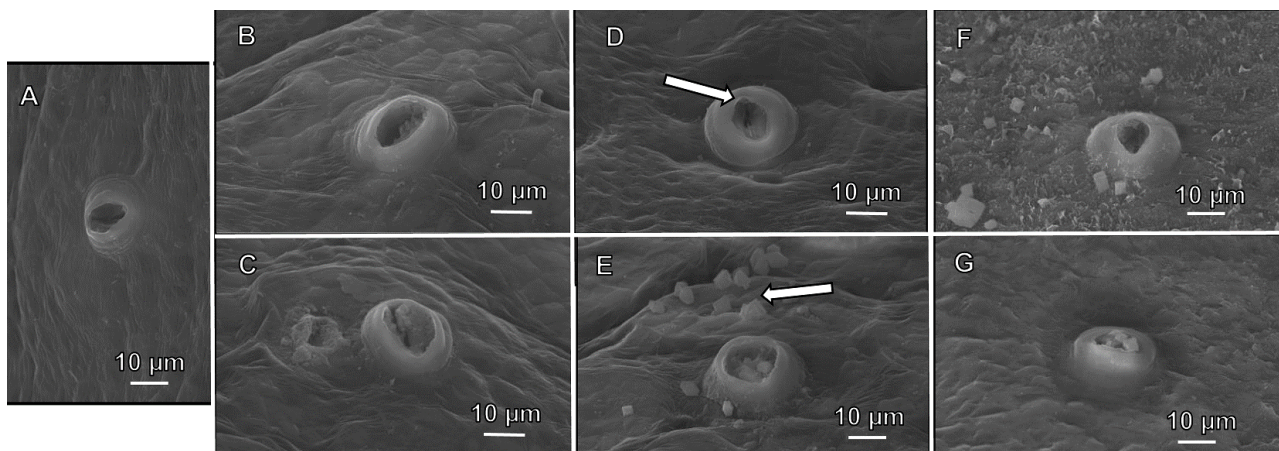


**Figure 2.** Scanning electron micrographs of stomata and the cuticle of orange fruits 30 (A), 44 (B,C), 66 (D,E), and 99 (F,G) days after full bloom (DAFB), showing healthy (A,B,D,F) and collapsed (C,F,G) stomata. Guard cells are distinguishable at 66 DAFB (arrow in D), scattered crystallized waxes (arrow in E) are also visible.

At 30 DAFB, stomata were fully developed in the fruits epidermis with a domed projection (crypt) over the guard cells. In this early phase, stomata appeared to be fully functional, and no plugs were observed (Figure 2A,B). From stage I of fruit development (>44 DAFB), there was a gradual occurrence of collapsed and plugged stomata occurred in the orange fruit surface, which increased with fruit maturity (Figure 2C,E,G). Some stomata were found to be covered with a closed crypt and epicuticular waxes (Figure 2C,E,G). No remarkable differences regarding fruit surface stomatal structure were found in stages I and II of fruit development.

At 44 DAFB, elongated bi-pyramidal crystalized wax structures started to appear on the fruit surface in considerable amounts, often forming clusters. These clusters became more common at 66 DAFB (Figure 2E). Few cracks in the rind surface could be observed at 30 DAFB and 44 DAFB, with no difference regarding crack size and frequency of appearance between both fruit developmental phases.

At 99 DAFB, during stage II of fruit development, two different wax structures were observed on the orange fruit surfaces. The first type (Figure 2F) were bipyramidal structures, with waxy substances of platelet forms covering most of the fruit surface. The second type showed a uniform amorphous material covering the fruit surface (Figure 2G). The amorphous and bipyramidal substances occurring at the orange fruit surface were chemically analyzed by SEM-EDX to determine their composition, which only contained carbon (C) and hydrogen (H) atoms, indicating they were true waxes. During stage I of fruit development, surface wax structures were heterogeneously present, with the occurrence of high density and low-density areas. Focusing on cuticle morphological development during the fruit set (30 DAFB), amorphous waxes were unevenly present in the fruit surface and covered only a small fraction of it (Figure 3A). At stage I of fruit development (44 DAFB), the surface area coverage of amorphous waxes increased (Figure 3B). At 30 DAFB and 44 DAFB, the orange fruit cuticle had a thickness of  $0.036 \pm 0.003 \mu\text{m}$  and  $0.038 \pm 0.003 \mu\text{m}$  (Figure 3C,D), respectively.

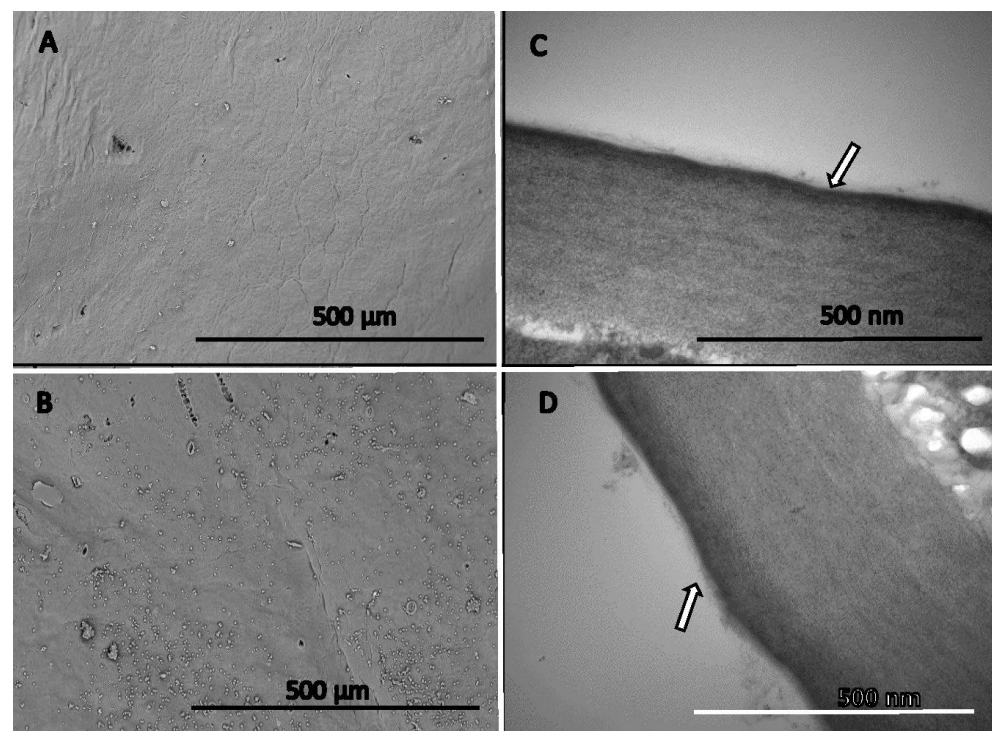


**Figure 3.** Scanning electron micrographs of orange fruit surfaces analyzed 30 (A) and 44 DAFB (B). Transmission electron micrographs of orange fruit epidermal cell wall and cuticle of fruits sampled 30 (C) and 44 DAFB (D). Arrows indicate the cuticle, and dark material underneath the cuticle corresponds to pectin.

### 3.3.2. Fruit Cross-Section Anatomy

To identify possible physical barriers for Ca transport with the fruit following fruit surface treatment with a Ca fertilizer; cross-sections were examined at different fruit phenological stages. As early as 30 DAFB (~7.58 mm fruit diameter) (Figure 4A,B), all the major structures of citrus fruit were already recognizable, namely: flavedo, albedo and pulp, and oil glands.

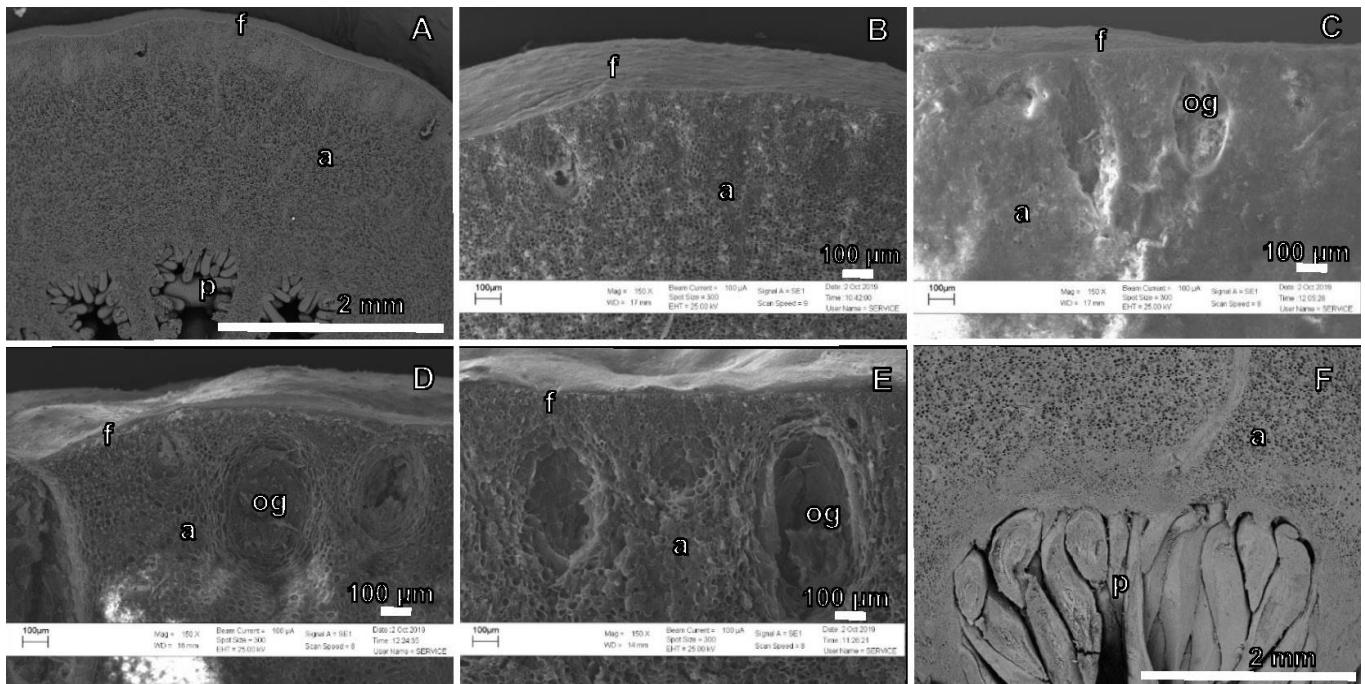


**Figure 4.** Cross-sections of orange fruits at different developmental stages with a focus on the albedo (a), flavedo (f), oil glands (og) and pulp (p). Micrographs correspond to 30 DAFB (A,B), 44 DAFB (C), 66 DAFB (D), and 99 DAFB (E,F).

Flavedo cells were smaller in size but had a higher density, occupying the zone immediately underneath the fruit surface and close to the larger and less dense albedo cells (Figure 4A,B). Juice sacs occupied a small fraction of the fruit during stage I (Figure 4A,B) and experienced a marginal size increase during this stage. Oil glands appeared as oval depressions near the fruit surface (Figure 4C–F) and were always found in the area between the flavedo and the albedo. The cells forming these glands are commonly long and stretched, being smaller in the flavedo area and larger in the albedo area. At 30 DAFB, some oil glands were recognizable, but the majority appeared from 44 DAFB onwards (~15.36 mm fruit diameter), oil glands increased in size, and the depression that they formed started to be more pronounced. Albedo cells were the largest and most abundant cells during stage I of fruit development, occupying most of the fruit volume (Figure 4A–D).

At 99 DAFB (stage II of fruit development ~48.77 mm fruit diameter), juice sacs were large, making the pulp the major fraction of the fruit relative to that of the albedo (Figure 4E,F).

Chloroplasts were found at the fruit set and stage I of development, most commonly in flavedo but also albedo cells (Figure 5). Albedo cells were larger in size than flavedo ones (Figure 5D versus Figure 5C).

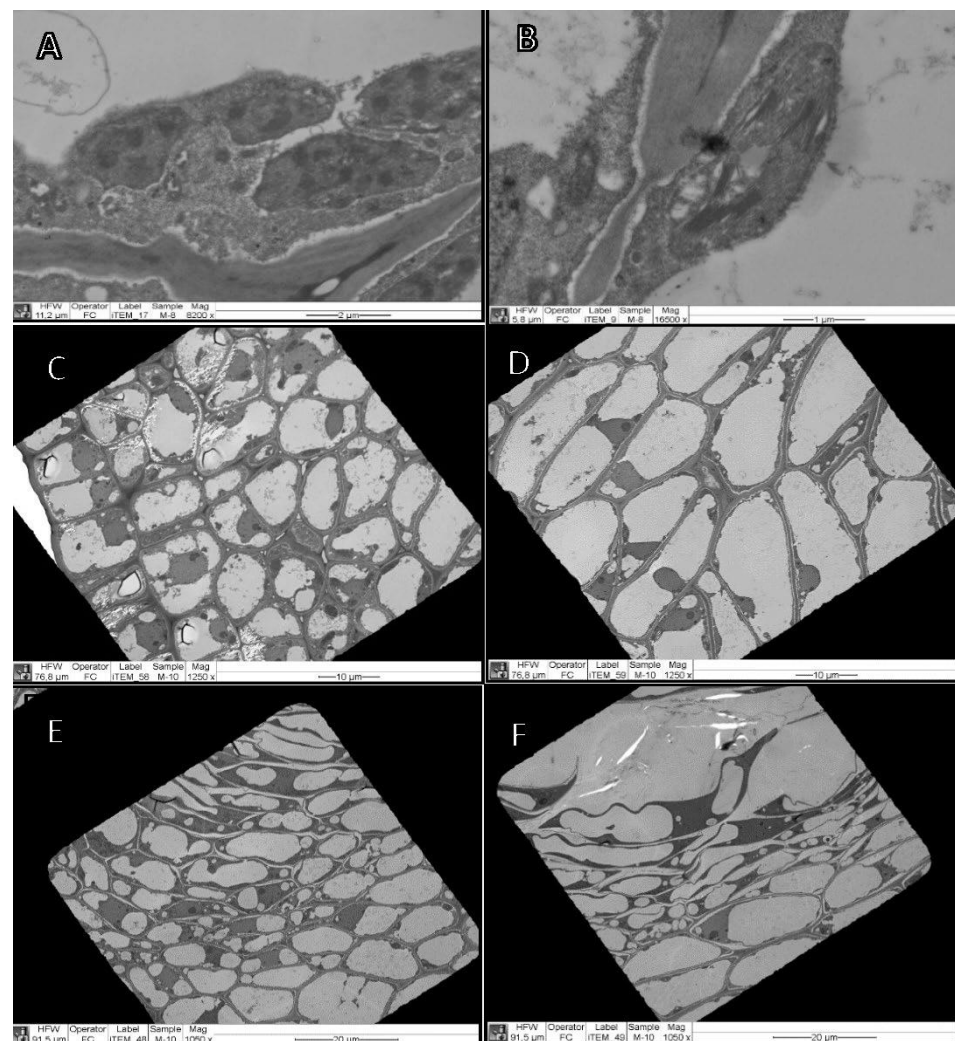


**Figure 5.** Transmission electron micrographs of orange fruits. Chloroplasts were found in flavedo (A,C) and albedo cells (B,D) of 30 DAFB fruits. Flavedo cells near an oil gland (E) and albedo cells near an oil gland (F) of 44 DAFB fruits.

### 3.3.3. Calcium Oxalate Crystals

Observations of fruit cross-sections revealed the presence of CaOx crystals from stage I of fruit development (44 DAFB). Crystals formed in the area of the flavedo and albedo but not in the pulp. These crystals were unevenly distributed (Figure 6A), showing an elongated bipyramidal shape with a square base (Figure 6B). Crystal clusters (CaOx) were frequently found around oil glands but not within them and were observed until mid-stage II of fruit development (99 DAFB). SEM-EDX was also used to determine the elemental composition of the crystals, which were always found to contain C, oxygen (O), and Ca, with the proportion of Ca sometimes reaching up to 42.08%. Fruits collected at different developmental stages were analyzed, also focusing on other structures close to the CaOx crystals, which were never found to contain Ca in their chemical composition.

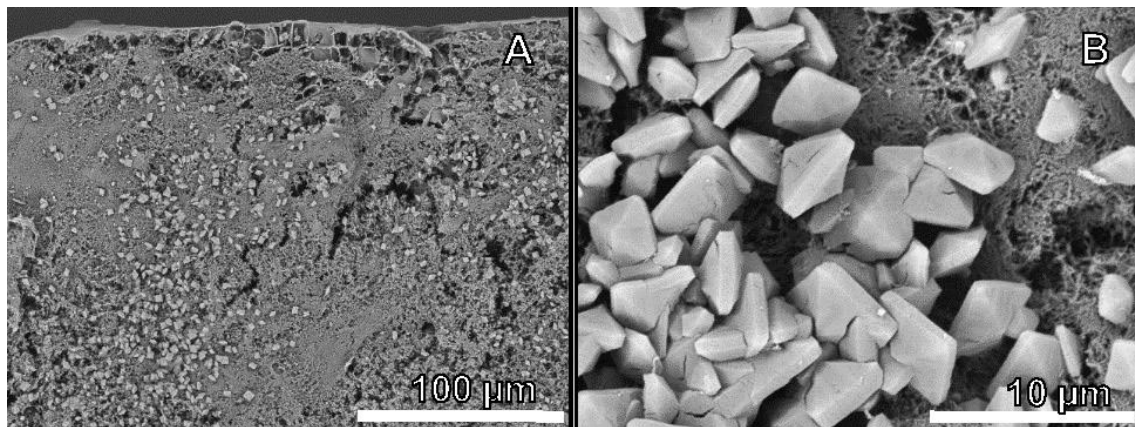


**Figure 6.** Scanning electron micrographs of calcium oxalate crystals found in 44 DAFB orange fruits. Oxalate crystal distribution in the fruit rind (A) and crystal morphology (B).

### 3.3.4. Pedicel Cross-Sections

In Figure 7, scanning electron micrographs of pedicel cross-section corresponding to 30 DAFB (diameter of  $1.34 \text{ mm} \pm 0.04$ ) and at 44 DAFB (diameter of  $2.29 \text{ mm} \pm 0.04$ ) are shown.

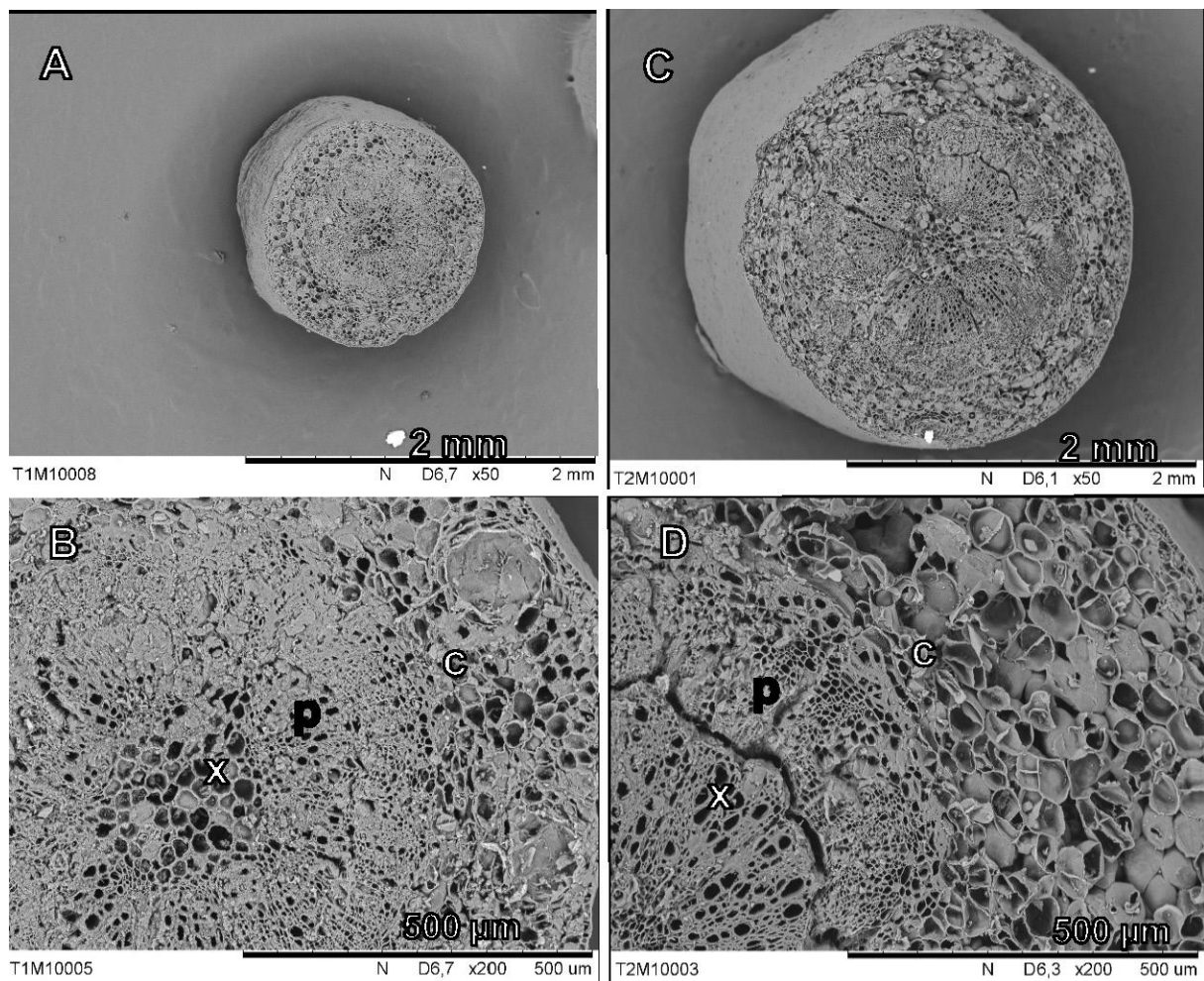


**Figure 7.** Pedicel cross-section ( $\times 50$ ) of 30 DAFB (A,B) and 44 DAFB (C,D) orange fruits observed by SEM. Entire cross-sections (A,C) and magnified images ( $\times 200$ ) (B,D) showing the xylem (x), phloem (p), and cortex (c).

Pedicle cross-sections significantly increased in the diameter between 30 and 44 DAFB (Figure 7A versus Figure 7C). At the fruit set (30 DAFB, Figure 7A,B), the xylem, phloem, and cortex can be distinguished, and these structures were increasing in size toward 44 DAFB (Figure 7B,D). (Figure 7. Scanning electron micrographs of pedicle cross-section cuts at 30 DAFB (A) and 44 DAFB (B). An overview (A1 and B1) and a magnified micrograph (A2 and B2) for the identification of xylem (x), phloem (p) and cortex (c).)

#### 4. Discussion

The success of foliar fertilization and fruit surface treatments depends on the absorption and mobility of the nutrients which are applied to the plant tissues. However, the effectiveness of foliar nutrient sprays can be variable because it depends on the interactions between environmental, physical, and chemical factors and also plant tissue anatomy [14]. In particular, Ca is a major essential nutrient that has a key structural role in the cell wall and membranes. Hence, Ca nutrition is associated with the quality and firmness of commercial fruits. Calcium transport depends on plant organ transpiration. Therefore, any factor which reduces transpiration can limit Ca transport from the roots to the leaves and/or fruits [7,44], and deficiency can develop in organs with low transpiration rates, such as fruits [1]. Subsequently, fruit surface treatments with Ca fertilizers supplied as sprays are often recommended as a 'potential tool to decrease the incidence of Ca-related disorders, and also for increasing fruit firmness, storability, and shelf-life' [1,45].

In this study,  $^{45}\text{Ca}$  was used as a tracer on different application dates to determine the absorption and mobilization of Ca supplied to the surface of fruits. The presence of this tracer in treated fruit tissues showed that the surface-applied Ca was absorbed in all the phases of fruit development evaluated (i.e., from fruit set to mid stage II). Citrus fruits have two morphologically distinct parts: the pericarp (i.e., the rind formed by flavedo + albedo) and the endocarp (i.e., the pulp) [46].

After  $^{45}\text{Ca}$  absorption, this tracer was transported from the fruit surface to the flavedo and albedo (Figure 1). This suggests that the morphological development of the rind during the period analyzed in this experiment was not a limiting factor for the transport of  $^{45}\text{Ca}$  from the surface to the fruit flavedo and albedo. However, the mobility of  $^{45}\text{Ca}$  to the pulp varied with the fruit phenological stage (i.e., with the different dates of Ca application). The highest partition rate of the  $^{45}\text{Ca}$  tracer reaching the pulp (39%) was recorded at the fruit set (30 DAFB), whereas in the other treatments, only between 17 and 19% of the tracer was recovered in this inner tissue. Some authors [46] indicated that in citrus fruits, the pulp is hydrolytically separated from the rind, which could partly explain our findings. Additionally, it must be considered that the rind of the fruit (mainly the albedo) experiences a great development after the fruit set, while the pulp in the same period shows minimal growth [22,25,26].

Before reaching the pulp, the surface absorbed  $^{45}\text{Ca}$  has to be transported through the flavedo and the albedo. The highest percentage of this tracer remained in the rind, reaching up to 81–83% for the supplied  $^{45}\text{Ca}$  amount when treatments were carried out after fruit set (i.e., at 44, 66, and 99 DAFB) (Figure 1). Out of this proportion, approximately 39 to 45% was found in the flavedo and 38 to 43% in the albedo of orange fruits.

From our results, it can be derived that fruit morphology (rind development) at the fruit set influences  $^{45}\text{Ca}$  distribution. Previous reports analyzed the development of the citrus peel and its main features, describing the increase in fruit size due to a high rate of cell multiplication and growth in these early developmental phases [22,25,26]. During these stages, the morphology and composition of tissues will change. The authors of [47] indicated that the most important factors for Ca efficiency are the timing of the application and the crop developmental stage.

Application of  $^{45}\text{Ca}$  during the fruit set period (30 DAFB) led to an increased  $^{45}\text{Ca}$  transport from the treated surface to the pulp in comparison to the other treatment dates (Figure 1). At the fruit set, the transpiration rate of the fruit is maximum, but it quickly

declines, whereas leaf transpiration is maintained at a greater rate [2]. In these early stages of fruit development, most of the  $\text{Ca}^{2+}$  is delivered to fruit [4,5].

Regarding Ca absorption and mobility, some studies highlight the development of stomata, cuticles, and oil glands, in addition, to the appearance of a discontinuity between the tissues of the rind and pulp [19,20,22,48]. It has also been reported that the fruit surface can influence the effectiveness of foliar fertilizer applications, mainly due to its chemical and structural nature [14], which can change during fruit development (Figures 4 and 6). Calcium spray absorption and mobilization may also be affected by other physiological aspects, such as mineral element homeostasis, plant water status, or the development of the pedicel. To identify the possible factors that affect the absorption and transport of surface applied  $^{45}\text{Ca}$ , different observations and analyses were carried out with orange fruits of different ages. Stomata were always found on the orange fruit surfaces (Figure 2), which were morphologically similar to the ones described for “Satsuma” mandarin fruits [20]. Orange fruit stomata were composed of a pair of guard cells protected by a crypt with a hole at the top. Stomata were morphologically intact in young fruits, but some gradually collapsed during fruit growth. In this study, stomatal collapse and plugging were observed at the early stages of fruit development and became more frequent over time (Figure 2).

It has been described that the density of fruit stomata is determined at anthesis, stomatal frequency decreasing during fruit expansion [20,49,50]. Thereby, for a fruit with a fully developed cuticle, the surface of open pores will be mainly determined by the occurrence of functional or collapsed stomata. In “Satsuma” mandarin, it has been reported that stomata grow from anthesis to approximately 88 DAFB with an increasing frequency of collapse, which is slow until 118 DAFB and more rapid up to 153 DAFB has been observed, with a proportion of more than 80%, occluded stomata at the mature stage [20]. The contribution of stomata to the absorption of fertilizer sprays can be highly significant, but many aspects associated with the uptake process are unclear to date [16]. No relationship has been found between stomatal density and citrus fruit transpiration [20], which suggests that stomatal absorption may be related to the functionality rather than the frequency of stomatal pores. In this study, the contribution of stomata to the absorption of  $^{45}\text{Ca}$  applied on to fruit surface from fruit set could not be quantified, but they may serve as uptake pathway through the cuticle towards the fruit interior.

In this work, it was found that all stomata were functional at the fruit set (30 DAFB) and began to collapse from 44 DAFB onwards, which coincided with the highest percentage of  $^{45}\text{Ca}$  found in the pulp when applied during the fruit set.

The cuticle has been described as a key barrier for the absorption of agrochemicals applied to the surface of fruits [51]. In this way, any opening through the cuticle may facilitate the absorption of nutrient sprays [14]. Epicuticular waxes of different morphology were detected at the surface of developing fruits, which began to appear from 44 DAFB in a sparse and dispersed way and were observed from 66 DAFB more frequently in groups or “clusters” (Figure 2). In the middle of phase II of fruit development (99 DAFB), two different epicuticular wax morphologies were found on orange fruit surfaces. The first was associated with bipyramidal and platelet-shaped structures covering the entire surface of the fruit, excepting stomata (Figure 2E), as described by other authors [19,20,52,53]. The second kind of waxes corresponded with a uniform amorphous layer (Figure 2G), as also described in some studies [19,54]. The different surfaces found for the same state of fruit development may be due to chemical and structural variations during cuticle development (Figure 3). In this sense, the effect on sun exposure has been described, with the shaded side having more crystalline structures than the exposed side, which presents more amorphous waxy structures [53,54]. These amorphous, platelet-shaped structures have been described for citrus fruits in similar fruit developmental stages [53,54]. SEM-EDS microanalysis of such fruit surface structures showed that they were composed of C as the main element and waxed. These results are consistent with previous descriptions of citrus fruits epicuticular waxes, which are mainly composed of fatty acids and derivatives [54].

Analysis of cuticle thickness observed in transmission electron microscopy (TEM) micrographs showed no significant differences between samples at 30 DAFB and 44 DAFB (Figure 3). This result is similar to previous reports with “Newhall” orange, which showed a significant development of the cuticle at approximately 120 DAFB [19]. The appearance of the fruit cuticle at 30 and 44 DAFB was similar, with the presence of scattered and sparse epicuticular waxes (Figure 3A,B). This result suggests that on both dates, there was a lower barrier effect to the absorption of surface applied  $^{45}\text{Ca}$ , which is also correlated with the subsequent Ca mobilization toward inner tissues of the fruit [39]. In addition, on both dates, stomata were fully developed, possibly favoring the process of foliar absorption of  $^{45}\text{Ca}$ .

The presence of these epicuticular waxes does not seem to be an impediment to the absorption of  $^{45}\text{Ca}$  during fruit set or phase I of fruit development. The greater development of epicuticular waxes after 44 DAFB did not result in differences in the distribution of  $^{45}\text{Ca}$  in the fruit. These findings suggest that cuticle development during fruit set (30 DAFB) and mid-phase II of fruit development (99 DAFB) had a weak or no effect on the absorption and transport of the  $^{45}\text{Ca}$  applied to the surface of fruits.

The chemical composition of the cuticle has been described for 60 DAFB “Newhall” oranges, mainly presenting fatty acids up to 120 DAFB [54,55]. After this date, the composition of the cuticle begins to change, and the content of fatty acids decreases in favor of aldehydes and alkanes. Both compounds have a positive correlation with water retention by the fruit, making it more impermeable. In contrast, fatty acids do not show this effect [19,54]. These studies point to the lower waterproofing capacity of the cuticle before its change in composition, which would occur late in phase II of fruit development. Hence, it is likely that during this experiment, the cuticle of fruits did not have a strong waterproofing layer which also limited the absorption of surface-applied  $^{45}\text{Ca}$ .

Observation of fruit cross-section by SEM showed incipient oil glands in the fruit rind during fruit set (30 DAFB), which became much more noticeable during phase I of fruit development (44 DAFB) (Figure 5). After this date, the oil glands continued to develop and increase in size, which has been reported in “Washington” navel oranges, mainly during phase I of fruit development, the stage of cell division, accompanied by an increased cell wall thickness of the perimeter cells of these glands [48]. The greater development of the oil glands at 44 DAFB is coincident with the lower delivery of  $^{45}\text{Ca}$  to the pulp during this date, compared to that at 30 DAFB. The greater presence of these glands in early phase I of fruit development may be an obstacle for the mobilization of  $^{45}\text{Ca}$  to the pulp. We hypothesize that the presence of oil glands in the orange rind could represent a barrier to the flow of Ca into the pulp (Figures 5 and 6).

Regarding the development of fruit tissues, the albedo is the largest fruit volume fraction from the fruit set to the end of phase I [22], constantly increasing its size between 30 DAFB and 66 DAFB. This larger size of the albedo would imply that the distance to the pulp increases significantly, which would also affect the transport of  $^{45}\text{Ca}$  to the pulp. In addition, morphological changes, such as the separation and discontinuity of the tissue from the albedo to the pulp (Figure 4A,B), may hinder Ca mobility. After the end of phase I of fruit development, the pulp grew at a high rate, increasing the separation of the rind with the pulp, being it the largest fraction of the fruit volume at 99 DAFB during mid-phase II of fruit development (Figure 4B). The maximum growth of the albedo has been described during phase I of the fruit, followed by an increase in the growth rate of the pulp juice vesicles as they approach phase II of fruit development [22,25,52].

It is possible that the increase in albedo growth during phase I of fruit development caused a lower mobilization of  $^{45}\text{Ca}$  in the rind due to the greater cellular activity occurring in these tissues and the consequent formation of several cellular structures that require Ca [1]. Additionally, there is a discontinuity between the tissues that hinder mobility [22]. It is also possible that the surface-applied  $^{45}\text{Ca}$  was diluted in the fruit of greater volume, as previously reported [5].

The concentration of unlabeled Ca in the fruit increased as fruit development progressed. On the other hand, the percentage of dry weight decreased (Table 2). At harvest, the orange rind showed a higher Ca concentration than the pulp.

In the fruit pedicel cross-sections, the xylem, phloem, and cortex were recognizable already at the fruit set (30 DAFB). A significant increase in the size between the fruit set and phase I of fruit development (44 DAFB) of all pedicel tissues was also observed (Figure 7). It has been reported in “Salustiana” orange that the transverse growth of the pedicel is determined by the growth of the xylem and phloem, which is also correlated with fruit growth [56].

The growth of the xylem area was coincident with the increase in fruit Ca concentration (Table 2). Several studies have suggested a relationship between the influx of Ca on the fruit and the functional area of the xylem in the pedicel [6,7,57]. This would mean that the growth after the fruit set would favor a greater influx and possibly a greater concentration of Ca in the fruit, which would be deposited in greater magnitude in the rind. However, vessel density, size, and area in the pedicel showed no correlation with the fruit Ca uptake rate [58].

Calcium oxalate crystals of a square-based bipyramidal morphology were found in fruit cross-sections from the beginning of phase I of fruit development until the end of this experiment (Figure 7). The crystals in orange fruits were found in the flavedo and albedo and showed high levels of Ca in their chemical composition on all dates of observation, which was corroborated by SEM-EDX. By contrast, the structures found did not contain Ca in their composition, indicating that they were epicuticular waxes. The consistency of crystal morphology has been reported as evidence for genetic regulation in the formation of these crystals. The plant seems to be able to regulate the environment in which the crystals develop, which is decisive for the final morphology of these crystals [28,33,59]. This square-bipyramidal morphology has been identified as CaOx dihydrate in different structures related to medicine, geology, and chemistry, in tissues such as living organisms, biogeochemical processes, or processes of artificial synthesis of CaOx crystals [59–62].

Voogt et al. [47] indicated that even after mineral element leaf absorption, the relevance of foliar fertilization to plant growth is unclear; some nutrients are not mobilized to other organs by binding to permanent structures where they are deposited. Calcium is a nutrient with low phloem mobility, and thus, once deposited in an organ, there is little to no redistribution [9]; e.g., once Ca is deposited in vacuoles, it is rarely redistributed [28].

The relationship between Ca and the development of different fruit tissues during the stages studied in this work has been described by several authors in different citrus species. In orange, the albedo is the tissue with the highest growth during phase I and presents the greatest influx of Ca to its cells, with a higher concentration of calcium in the rind than in the pulp, which at this stage has minimal development [6,22].

Regarding the evolution of Ca concentrations at different fruit developmental stages, Ca concentration was lower at the fruit set (30 DAFB) than that at stage I (44 DAFB) (Table 2), in which it showed a significant increase that coincided with the appearance of CaOx crystals. Calcium concentrations showed a peak at the end of stage I (66 DAFB) and harvest; this study showed a decreased rate of Ca accumulation [63]. The formation of CaOx crystals could indicate that at this fruit developmental stage, the Ca level was sufficient, and with a higher quantity, the plant regulated cytosolic Ca through the mechanisms of sequestration of calcium in the vacuole as crystals [32,33,37].

The occurrence of CaOx crystals only in the flavedo and albedo issues suggests that their presence is related to the higher concentration of Ca existing in both tissues. At no dates were CaOx crystals found in the pulp, which is a tissue with relatively lower Ca concentrations, as previously reported [30].

The concentration of Ca in the pedicel was always higher (between 2 and 9 times) than in the fruit, a “bottleneck” effect of pedicels on the mobilization of Ca from plant to fruit has been described, which would cause the high concentration differences between the two [58]. The Ca concentration found in this study supports the possible bottleneck

effect of pedicels, as the concentrations were different from fruit set to mid-phase II of fruit development.

## 5. Conclusions

The fruits of orange cv. Fukumoto absorbed  $^{45}\text{Ca}$  after fruit surface applications which were carried out at different stages of fruit development, namely: fruit set (30 DAFB), phase I of fruit growth (44 DAFB), end of phase I (66 DAFB), and mid-phase II (99 DAFB). The distribution of  $^{45}\text{Ca}$  when applied during the fruit set period (30 DAFB) was significantly different when compared to that of the other treatments, with 61% in the rind and 39% in the pulp. Regarding the transport of  $^{45}\text{Ca}$  applied at 44, 66, and 99 DAFB, 81–83% remained in the rind, and between 17 and 19% reached the pulp.

After tissue SEM analysis, it was observed that the  $^{45}\text{Ca}$  absorption and transport results were coincident with the development of oil glands, the increase in the diameter of the pedicel, the appearance of  $\text{CaOx}$  crystals, and an increase in the fruit size due to the growth of the albedo, increasing the distance to the pulp. Stomata were defined on the fruit surface, and as the season advanced, a greater number of collapsed ones were observed. On the other hand, the cuticle of the fruit surface did not impede surface-applied  $^{45}\text{Ca}$  absorption in the developmental stages of the fruit studied.

The distribution of  $^{45}\text{Ca}$  found in treated fruits at the fruit set (30 DAFB) led to significant differences in the mobilization of the exogenous Ca toward the pulp. This result suggests that once the structures of the oil glands have been formed and the pulp tissue was differentiated, it is difficult to reach that tissue; i.e., the influx of Ca into the pulp is reduced by physical impediments, more distance between rind and pulp and sequestration of Ca as  $\text{CaOx}$ .

The presence of  $\text{CaOx}$  crystals was coincident with an increase in the concentration of Ca in the fruit and lower mobility of foliar  $^{45}\text{Ca}$  toward the pulp. The fruit Ca concentration increased from the fruit set, 30 DAFB to 99 DAFB. From the first date, the pedicel showed the formation of xylem, phloem, and cortex, and its Ca concentration was always greater than that of the fruit.

The information obtained in this study may be essential for improving Ca fertilizer efficacy in citrus because it can help optimize foliar/surface-applied Ca absorption and transport in fruit tissues and design suitable fertilizer programs and spray application methods.

**Author Contributions:** Conceptualization, C.B. and J.M.; methodology, C.B., J.M., X.V., X.R.-S. and A.N.; validation, C.B., J.M., X.V., X.R.-S. and A.N.; formal analysis, C.B., F.C. and J.M.; investigation, C.B., F.C. and J.M.; resources, C.B., F.C. and J.M.; data curation, C.P., C.B. and J.M.; writing—original draft preparation, C.B., V.F. and F.C.; writing—review and editing, C.B., C.P. and J.M.; visualization, C.B., V.F.; supervision, C.B. and J.M.; project administration, J.M.; funding acquisition, J.M. and C.B. All authors have read and agreed to the published version of the manuscript.

**Funding:** This research received no external funding.

**Institutional Review Board Statement:** Not Applicable.

**Informed Consent Statement:** Not Applicable.

**Data Availability Statement:** The data presented in this study are available on request from the corresponding author.

**Acknowledgments:** The authors acknowledge Agrícola El Cruce for providing the physical location for the field trial.

**Conflicts of Interest:** The authors declare no conflict of interest.

## References

1. White, P.J.; Broadley, M.R. Calcium in plants. *Ann. Bot.* **2003**, *92*, 487–511. [[CrossRef](#)]
2. Hocking, B.; Tyerman, S.D.; Burton, R.A.; Gilliam, M. Fruit calcium: Transport and physiology. *Front. Plant Sci.* **2016**, *7*, 569. [[CrossRef](#)] [[PubMed](#)]
3. Li, J.; Chen, J. Citrus Fruit-Cracking: Causes and Occurrence. *Hortic. Plant J.* **2017**, *3*, 255–260. [[CrossRef](#)]
4. Montanaro, Y.; Dichio, B.; Xiloyannis, C. Significance of fruit transpiration on calcium nutrition in developing apricot fruit. *J. Plant Nutr. Soil Sci.* **2010**, *173*, 618–622. [[CrossRef](#)]
5. Montanaro, G.; Dichio, B.; Lang, A.; Mininni, A.N.; Nuzzo, V.; Clearwater, M.J.; Xiloyannis, C. Internal versus external control of calcium nutrition in kiwifruit. *J. Plant Nutr. Soil Sci.* **2014**, *177*, 819–830. [[CrossRef](#)]
6. Storey, R.; Treeby, M.T. Nutrient uptake into navel oranges during fruit development. *J. Hortic.* **2002**, *77*, 91–99. [[CrossRef](#)]
7. de Freitas, S.T.; Mitcham, E.J. Factors involved in fruit calcium deficiency disorders. *Hortic. Rev. (Am. Soc. Hortic. Sci.)* **2012**, *40*, 107–146. [[CrossRef](#)]
8. Saure, M.C. Why calcium deficiency is not the cause of blossom-end rot in tomato and pepper fruit—a reappraisal. *Sci. Hortic.* **2014**, *174*, 151–154. [[CrossRef](#)]
9. Saure, M.C. Calcium translocation to fleshy fruit: Its mechanism and endogenous control. *Sci. Hortic.* **2005**, *105*, 65–89. [[CrossRef](#)]
10. Winkler, A.; Knoche, M. Calcium and the physiology of sweet cherries: A review. *Sci. Hortic.* **2019**, *245*, 107–115. [[CrossRef](#)]
11. Treeby, M.T.; Storey, R. Calcium-spray treatments for ameliorating albedo breakdown in navel oranges. *Aust. J. Exp. Agric.* **2002**, *42*, 495–502. [[CrossRef](#)]
12. Agustí, M.; Martínez-Fuentes, A.; Mesejo, C. Citrus fruit quality. physiological basis and techniques of improvement. *Agrociencia* **2002**, *6*, 1–16.
13. Bonomelli, C.; Fernández, V.; Martiz, J.; Videla, X.; Arias, M.I.; Rojas-Silva, X.; Nario, A. Absorption and distribution of root, fruit and foliar applied  $^{45}\text{Ca}$  in “Clemenules” mandarin trees. *J. Sci. Food Agric.* **2020**, *100*, 4643–4650. [[CrossRef](#)]
14. Fernández, V.; Sotiropoulos, T.; Brown, P. *Foliar Fertilization: Scientific Principles and Field Practices*, 1st ed.; IFA: Paris, France, 2013. [[CrossRef](#)]
15. Li, C.; Wu, J.; Blamey, F.; Wang, L.; Zhou, L.; Paterson, D.J.; Van der Ent, A.; Fernández, V.; Lombi, E.; Wang, Y.; et al. Non-glandular trichomes of sunflower are important in the absorption and translocation of foliar-applied Zn fertilizer. *J. Exp. Bot.* **2021**, *72*, 5079–5092. [[CrossRef](#)] [[PubMed](#)]
16. Eichert, T.; Kurtz, A.; Steiner, U.; Goldbach, H.E. Size exclusion limits and lateral heterogeneity of the stomatal foliar uptake pathway for aqueous solutes and water-suspended nanoparticles. *Physiol. Plant* **2008**, *134*, 151–160. [[CrossRef](#)] [[PubMed](#)]
17. Fernández, V.; Gil-Pelegrín, E.; Eichert, T. Foliar water and solute absorption: An update. *Plant J.* **2021**, *105*, 870–883. [[CrossRef](#)]
18. Schönherr, J. Calcium chloride penetrates plant cuticles via aqueous pores. *Planta* **2000**, *212*, 112–118. [[CrossRef](#)]
19. Wang, J.; Sun, L.; Xie, L.; He, Y.; Luo, T.; Sheng, L.; Luo, Y.; Zeng, Y.; Xu, J.; Deng, X.; et al. Regulation of cuticle formation during fruit development and ripening in “Newhall” navel orange (*Citrus sinensis* Osbeck) revealed by transcriptomic and metabolomic profiling. *Plant Sci.* **2016**, *243*, 131–144. [[CrossRef](#)]
20. Hiratsuka, S.; Suzuki, M.; Nishimura, H.; Nada, K. Fruit photosynthesis in Satsuma mandarin. *Plant Sci.* **2015**, *241*, 65–69. [[CrossRef](#)]
21. Storey, R.; Treeby, M.T. The morphology of epicuticular wax and albedo cells of orange fruit in relation to albedo breakdown. *J. Hortic. Sci.* **1994**, *69*, 329–338. [[CrossRef](#)]
22. Agustí Fonfría, M. *Citricultura*, 1st ed.; Mundi-Prensa: Madrid, España, 2000.
23. Alquezar, B.; Mesejo, C.; Alferez, F.; Agustí, M.; Zacarias, L. Morphological and ultrastructural changes in peel of ‘Navelate’ oranges in relation to variations in relative humidity during postharvest storage and development of peel pitting. *Postharvest Biol. Technol.* **2010**, *56*, 163–170. [[CrossRef](#)]
24. Tadeo, F.R.; Moya, J.L.; Iglesias, D.; Talón, M.; Primo-Millo, E. *Histología y Citología de Cítricos*, 1st ed.; Generalitat Valenciana: Valencia, España, 2003.
25. Spiegel-Roy, P.; Goldschmidt, E. *The Biology of Citrus*, 1st ed.; Cambridge University Press: Cambridge, UK, 1996.
26. Iglesias, D.J.; Cercós, M.; Colmenero-Flores, J.M.; Naranjo, M.A.; Ríos, G.; Carrera, E.; Ruiz-Rivero, O.; Lliso, I.; Morillon, R.; Tadeo, F.R.; et al. Physiology of citrus fruiting. *Braz. J. Plant Physiol.* **2007**, *19*, 333–362. [[CrossRef](#)]
27. Bonomelli, C.; Bravo, K.; Vega, A.; Ruiz, R.; Montenegro, G. Use of fura 2 fluorescent dyes as indicator for studying calcium distribution in several plant tissues. *Commun. Soil Sci. Plant Anal.* **2010**, *41*, 1061–1072. [[CrossRef](#)]
28. Franceschi, V.R.; Nakata, P.A. Calcium oxalate in plants: Formation and Function. *Annu. Rev. Plant Biol.* **2005**, *56*, 41–71. [[CrossRef](#)]
29. Storey, R.; Treeby, M.T. Cryo-SEM study of the early symptoms of peteca in “Lisbon” lemons. *J. Hortic. Sci. Biotechnol.* **2002**, *77*, 551–556. [[CrossRef](#)]
30. Undurraga, P.L.; Olaeta, J.A.; Retamales, J.B.; Escobar, J.; Toso, A.M. Effect of maturity and storage temperature on the development of peteca in lemons (*Citrus limon* (L.) Burm. F.) cv. Eureka. *Sci. Hortic.* **2009**, *122*, 56–61. [[CrossRef](#)]
31. Kostman, T.A.; Franceschi, V.R.; Nakata, P.A. Endoplasmic reticulum sub-compartments are involved in calcium sequestration within raphide crystal idioblasts of *Pistia stratiotes* L. *Plant Sci.* **2003**, *165*, 205–212. [[CrossRef](#)]
32. Nakata, P.A. Plant calcium oxalate crystal formation, function, and its impact on human health. *Front. Biol.* **2012**, *7*, 254–266. [[CrossRef](#)]

33. Webb, M.A. Cell-Mediated Crystallization of Calcium Oxalate in Plants. *Plant Cell* **1999**, *11*, 751. [[CrossRef](#)]
34. Ho, L.C.; Belda, R.; Brown, M.; Andrews, J.; Adams, P. Uptake and transport of calcium and the possible causes of blossom-end rot in tomato. *J. Exp. Bot.* **1993**, *44*, 509–518. [[CrossRef](#)]
35. Li, W.; Xu, F.; Chen, S.; Zhang, Z.; Zhao, Y.; Jin, Y.; Li, M.; Zhu, Y.; Liu, Y.; Yang, Y.; et al. A comparative study on Ca content and distribution in two Gesneriaceae species reveals distinctive mechanisms to cope with high rhizospheric soluble calcium. *Front. Plant Sci.* **2014**, *5*, 647. [[CrossRef](#)] [[PubMed](#)]
36. Lötscher, M.; Hay, M.J.M. Distribution of phosphorus and calcium from nodal roots of *Trifolium repens*: The relative importance of transport via xylem or phloem. *New Phytol.* **1996**, *133*, 445–452. [[CrossRef](#)]
37. Volk, G.M.; Goss, L.J.; Franceschi, V.R. Calcium channels are involved in calcium oxalate crystal formation in specialized cells of *Pistia stratiotes* L. *Ann. Bot.* **2004**, *93*, 741–753. [[CrossRef](#)]
38. Bonomelli, C.; Alcalde, C.; Aguilera, C.; Videla, X.; Rojas-Silva, X.; Nario, A.; Fernández, V. Absorption and mobility of radio-labelled calcium in chili pepper plants and sweet cherry trees. *Sci. Agric.* **2021**, *78*, 1–7. [[CrossRef](#)]
39. Kalcsits, L.; van der Heijden, G.; Reid, M.; Mullin, K. Calcium absorption during fruit development in ‘honeycrisp’ apple measured using <sup>44</sup>Ca as a stable isotope tracer. *HortScience* **2017**, *52*, 1804–1809. [[CrossRef](#)]
40. Videla, X.; Rojas-Silva, X.; Nario, A.; Arias, M.I.; Bonomelli, C. Calcination Method of <sup>45</sup>Ca Samples for Isotope Ratio Analysis via Liquid Scintillation. *Commun. Soil Sci. Plant Anal.* **2019**, *50*, 412–420. [[CrossRef](#)]
41. Cao, H.; Zhang, J.; Xu, J.; Ye, J.; Yun, Z.; Xu, Q.; Xu, J.; Deng, X. Comprehending crystalline  $\beta$ -carotene accumulation by comparing engineered cell models and the natural carotenoid-rich system of citrus. *J. Exp. Bot.* **2012**, *63*, 4403–4417. [[CrossRef](#)]
42. Rueden, C.T.; Schindelin, J.; Hiner, M.C.; DeZonia, B.E.; Walter, A.E.; Arena, E.T.; Eliceiri, K.W. ImageJ2: ImageJ for the next generation of scientific image data. *BMC Bioinform.* **2017**, *18*, 1–26. [[CrossRef](#)]
43. Di Renzo, J.A.; Casanoves, F.; Balzarini, M.G.; Gonzalez, L.; Tablada, M.; Robledo, C.W. *InfoStat Versión 2011*; Grupo InfoStat FCA: Córdoba, Argentina, 2011.
44. Bonomelli, C.; Gil, P.M.; Schaffer, B. Effect of soil type on calcium absorption and partitioning in young avocado (*Persea americana* Mill.) Trees. *Agronomy* **2019**, *9*, 837. [[CrossRef](#)]
45. Madani, B.; Wall, M.; Mirshekari, A.; Bah, A.; Mohamed, M.T.M. Influence of Calcium Foliar Fertilization on Plant Growth, Nutrient Concentrations, and Fruit Quality of Papaya. *Am. Soc. Hort. Sci.* **2015**, *25*, 496–504. [[CrossRef](#)]
46. Cronje, P.J.; Barry, G.H.; Huysamer, M. Fruiting position during development of ‘Nules Clementine’ mandarin affects the concentration of K, Mg and Ca in the flavedo. *Sci. Hortic.* **2011**, *130*, 829–837. [[CrossRef](#)]
47. Voogt, W.; Blok, C.; Eveleens, B.; Marcelis, L.; Bindraban, P.S. Foliar fertilizer application. In *VFRC Report 2013/2*; Virtual Fertilizer Research Center: Washington, DC, USA, 2013; Volume 43. [[CrossRef](#)]
48. Knight, T.G.; Klieber, A.; Sedgley, M. The relationship between oil gland and fruit development in Washington Navel orange (*Citrus sinensis* L. Osbeck). *Ann. Bot.* **2001**, *88*, 1039–1047. [[CrossRef](#)]
49. Hetherington, A.M.; Woodward, F.I. The role of stomata in sensing and driving environmental change. *Nature* **2003**, *424*, 901–908. [[CrossRef](#)] [[PubMed](#)]
50. Hieke, S.; Menzel, C.M.; Ludders, P. Effects of leaf, shoot and fruit development on photosynthesis of lychee trees (*Litchi chinensis*). *Tree Physiol.* **2002**, *22*, 955–961. [[CrossRef](#)]
51. Fernández, V.; Bahamonde, H.A.; Javier Peguero-Pina, J.; Gil-Pelegrín, E.; Sancho-Knapik, D.; Gil, L.; Goldbach, H.E.; Eichert, T. Physico-chemical properties of plant cuticles and their functional and ecological significance. *J. Exp. Bot.* **2017**, *68*, 5293–5306. [[CrossRef](#)]
52. Agustí, M.; Almela, V.; Juan, M.; Alferez, F.; Tadeo, F.R.; Zacarías, L. Histological and physiological characterization of rind breakdown of “Navelate” sweet orange. *Ann. Bot.* **2001**, *88*, 415–422. [[CrossRef](#)]
53. El-Otmani, M.; Arpaia, M.L.; Coggins, C.W.; Pehrson, J.E.; O’Connell, N.V. Developmental changes in “Valencia” orange fruit epicuticular wax in relation to fruit position on the tree. *Sci. Hortic.* **1989**, *41*, 69–81. [[CrossRef](#)]
54. Wang, J.; Hao, H.; Liu, R.; Ma, Q.; Xu, J.; Chen, F.; Cheng, Y.; Deng, X. Comparative analysis of surface wax in mature fruits between Satsuma mandarin (*Citrus unshiu*) and “Newhall” navel orange (*Citrus sinensis*) from the perspective of crystal morphology, chemical composition and key gene expression. *Food Chem.* **2014**, *153*, 177–185. [[CrossRef](#)] [[PubMed](#)]
55. Liu, D.C.; Zeng, Q.; Ji, Q.X.; Liu, C.F.; Liu, S.B.; Liu, Y. A comparison of the ultrastructure and composition of fruits’ cuticular wax from the wild-type “Newhall” navel orange (*Citrus sinensis* [L.] Osbeck cv. Newhall) and its glossy mutant. *Plant Cell Rep.* **2012**, *31*, 2239–2246. [[CrossRef](#)]
56. Laskowski, L.E.; Monerri, C.; García-Luis, A.; Guardiola, J.L. Vascularización del pedicelo y crecimiento del fruto de *Citrus sinensis* var. Salustiana y su relación con el contenido de ácido indolacético. *Bioagro* **2008**, *20*, 11–20.
57. Miqueloto, A.; do Amarante, C.V.T.; Steffens, C.A.; dos Santos, A.; Mitcham, E. Relationship between xylem functionality, calcium content and the incidence of bitter pit in apple fruit. *Sci. Hortic.* **2014**, *165*, 319–323. [[CrossRef](#)]
58. Song, W.; Yi, J.; Kurniadinata, O.F.; Wang, H.; Huang, X. Linking fruit Ca uptake capacity to fruit growth and pedicel anatomy, a cross-species study. *Front. Plant Sci.* **2018**, *9*, 1–11. [[CrossRef](#)]
59. Liu, Y.; Mao, H.; Liu, X.; Qiao, L.; Guo, R. Calcium oxalate crystallization in the presence of amphiphilic phosphoproteins. *Cryst. Eng. Comm.* **2014**, *16*, 8841–8851. [[CrossRef](#)]
60. Mathonnet, M.; Dessombz, A.; Bazin, D.; Weil, R.; Frédéric, T.; Pusztaszeri, M.; Daudon, M. Chemical diversity of calcifications in thyroid and hypothetical link to disease. *Comptes Rendus Chim.* **2016**, *19*, 1672–1678. [[CrossRef](#)]

61. Saffo, M.B.; Lowenstam, H.A. Calcareous deposits in the renal sac of a molgulid tunicate. *Science* **1978**, *200*, 1166–1168. [[CrossRef](#)] [[PubMed](#)]
62. Sturm, E.V.; Frank-Kamenetskaya, O.; Vlasov, D.; Zelenskaya, M.; Sazanova, K.; Rusakov, A.; Kniep, R. Crystallization of calcium oxalate hydrates by the interaction of calcite marble with fungus *Aspergillus Niger*. *Am. Mineral.* **2015**, *100*, 2559–2565. [[CrossRef](#)]
63. Storey, R.; Treeby, M.T. Seasonal changes in nutrient concentrations of navel orange fruit. *Sci. Hortic.* **2000**, *84*, 67–82. [[CrossRef](#)]